

Mean First Passage Times and Eyring-Kramers formula for Fluctuating Hydrodynamics

Jingbang Liu

Mathematics Institute, University of Warwick, Coventry CV4 7AL, United Kingdom
Department of Mathematics, University of Oslo, Oslo, 0851, Norway

E-mail: jingbanl@uio.no

James E. Sprittles

Mathematics Institute, University of Warwick, Coventry CV4 7AL, United Kingdom

E-mail: J.E.Sprittles@Warwick.ac.uk

Tobias Grafke

Mathematics Institute, University of Warwick, Coventry CV4 7AL, United Kingdom

E-mail: T.Grafke@warwick.ac.uk

Abstract. Thermally activated phenomena in physics and chemistry, such as conformational changes in biomolecules, liquid film rupture, or ferromagnetic field reversal, are often associated with exponentially long transition times described by Arrhenius' law. The associated subexponential prefactor, given by the Eyring-Kramers formula, has recently been rigorously derived for systems in detailed balance, resulting in a sharp limiting estimate for transition times and reaction rates. Unfortunately, this formula does not trivially apply to systems with conserved quantities, which are ubiquitous in the sciences: The associated zeromodes lead to divergences in the prefactor. We demonstrate how a generalised formula can be derived, and show its applicability to a wide range of systems, including stochastic partial differential equations from fluctuating hydrodynamics, with applications in rupture of nanofilm coatings and social segregation in socioeconomics.

1. Introduction

Metastability is a well-known phenomenon appearing in many areas of natural sciences: A stochastic system spends a long time near some typical configuration, but can rarely switch (transition) to a drastically different configuration. The corresponding waiting times are known to be exponentially large in the noise strength.

The typical picture is that of a stochastic diffusion in a potential landscape, where local minima correspond to long-lived states. Fluctuations can then push the system across a potential barrier into another local minimum, in which it will remain for long times. While chemical reactions, conformational changes in biomolecules, protein folding, or magnetic field reversal in ferromagnets are well-known examples of this phenomenon, similar ideas can be found in rather broad areas of science, such as in brain activity [1], tipping points in Earth's climate [2] including warm-water currents in the north Atlantic [3], or ecosystem collapse [4].

Concretely, take the gradient diffusion for $X_t \in \mathbb{R}^n$,

$$dX_t = -\nabla U(X_t) dt + \sqrt{2\varepsilon} dW_t, \quad (1)$$

where $U : \mathbb{R}^n \rightarrow \mathbb{R}$ is the potential, and W_t white-in-time Brownian motion. For this system and in the limit of small noise, $\varepsilon \rightarrow 0$, transitions between two local minima x_- and x_+ of $U(x)$ always happen through a saddle point x_s , and the expected transition time τ is given by the *Eyring-Kramers* formula

$$\tau = \frac{2\pi}{|\lambda_-|} \sqrt{\frac{|\det H_s|}{\det H_-}} e^{\Delta U/\varepsilon} \quad (2)$$

asymptotically sharp in the limit of vanishing ε . Here, $H_- = \nabla \nabla U(x_-)$ and $H_s = \nabla \nabla U(x_s)$ are the Hessian of the potential U at the starting fixed point x_- and at the saddle x_s , respectively, and λ_- is the single negative eigenvalue of H_s , corresponding to the single unstable direction of the saddle point. The exponential scaling with the energy barrier height $\Delta U = U(x_s) - U(x_-)$ is known as *Arrhenius' law* [5], and can be made rigorous within sample path large deviation theory as established in [6] in more general cases than just gradient diffusions. The pre-exponential factor is also known for almost a century [7, 8], but has only recently been proven rigorously [9, 10, 11, 12, 13]. Within these works, it is possible to consider the more general case of a diffusion in a potential landscape with *mobility* $M(x) : \mathbb{R}^n \rightarrow \mathbb{R}^{n \times n}$, which is positive definite and symmetric, via

$$dX_t = -M(X_t) \nabla U(X_t) dt + \varepsilon \nabla \cdot M(X_t) + \sqrt{2\varepsilon} M_{1/2}(X_t) dW_t, \quad (3)$$

where $M_{1/2}(x) : \mathbb{R}^n \rightarrow \mathbb{R}^{n \times n}$ is the unique positive definite matrix for which $M_{1/2} M_{1/2}^T = M$ and $\nabla \cdot M(x) = \sum_i \partial_{x_i} M_{ij}(x)$. In this case, the Eyring-Kramers formula reads

$$\tau = \frac{2\pi}{\mu_-} \sqrt{\frac{|\det H_s|}{\det H_-}} e^{\Delta U/\varepsilon}, \quad (4)$$

where μ_- is the unique negative eigenvalue of the matrix $M(x_s)H_s$.

While the generalised gradient diffusion with mobility (3) can still be interpreted as system that minimises the potential U , just with a position dependent metric given by the mobility, it opens up a much wider class of physical phenomena beyond the overdamped Langevin equation (1). In particular, if further generalizing to the functional setup and allowing generalised gradient diffusions in function spaces or spaces of probability measures, it includes hydrodynamic limits of interacting particle systems, lattice gases, pedestrian dynamics, traffic flow, etc, all of which can be seen as (functional) gradient flows of some entropy functional for a (generalised) Wasserstein metric [14]. For example, the large number of particles limit of many non-interacting random walkers is given by the stochastic diffusion equation for a density $\rho(x, t)$,

$$\partial_t \rho = \Delta \rho + \sqrt{2\varepsilon} \nabla \cdot (\sqrt{\rho} \eta),$$

with η spatio-temporal white noise, and $\varepsilon = 1/N$ for N random walkers. It can be interpreted as a functional gradient flow

$$\partial_t \rho = -M(\rho) \frac{\delta E[\rho]}{\delta \rho} + \sqrt{2\varepsilon} M_{1/2}(\rho) \eta \quad (5)$$

in the entropy landscape

$$E[\rho] = \int \rho \log \rho \, dx$$

and with mobility operator

$$M(\rho) \xi = \nabla \cdot (\rho \nabla \xi) \quad (6)$$

(and thus $M_{1/2}(\rho) \xi = \nabla \cdot (\sqrt{\rho} \xi)$). The main point of this paper is to generalise the Eyring-Kramers formula (4) to generalised gradient systems (5) with conserved quantities.

1.1. Main Result

The major problem in applying the Eyring-Kramers formula (4) to generalised gradient systems of the form (5) is that in almost all cases of physical relevance, the mobility operator is not positive definite, but instead features zero-eigenvalues corresponding to conserved quantities. For example the mobility in (6) has a zero eigenvalue, with constant functions being the corresponding eigenfunctions, that is associated with conservation of particle number for the underlying particle diffusion equation. This situation is generic in hydrodynamic limits, which often conserve mass, momentum, energy, etc. Our main result is a modification to the Eyring-Kramers formula, which corrects for the conserved quantity. It is given by

$$\tau = \frac{\pi}{\mu_-} \sqrt{\frac{|\det H_s|}{\det H_-}} \sqrt{\frac{\hat{m} \cdot H_s^{-1} \hat{m}}{\hat{m} \cdot H_-^{-1} \hat{m}}} e^{\Delta U/\varepsilon} \quad (7)$$

where \hat{m} is the vector normal to the conserved quantity submanifold, and where stable fixed point x_- and saddle point x_s have to be appropriately re-interpreted.

In the following, we will derive equation (7) via a formal asymptotic expansion. In particular, we will compute the asymptotics of the mean first passage time in section 2 through a boundary layer analysis and Laplace asymptotics, incorporating the complications of the conserved quantity. We will then demonstrate the applicability of the formula by computing mean first passage times for a simple toy model in section 3, and to two more realistic stochastic partial differential equations describing liquid thin film rupture in section 4, and urban segregation in a socioeconomic model of social dynamics in section 5.

2. Mean First Passage Time and Laplace Asymptotics

Consider first the general stochastic differential equation for $X_t \in \mathbb{R}^n$,

$$dX_t = b(X_t) dt + \varepsilon \sigma(X_t) dW_t, \quad (8)$$

where $b : \mathbb{R}^n \rightarrow \mathbb{R}^n$ is the deterministic drift, $\sigma : \mathbb{R}^n \rightarrow \mathbb{R}^{n \times n}$ defines the noise covariance matrix $a(x) = \sigma(x)\sigma^T(x)$, and W_t is n -dimensional Brownian motion. We assume the case where there is a stable fixed point $x_- \in \mathbb{R}^n$ such that $b(x_-) = 0$ and the eigenvalues of $\nabla b(x_-)$ all have negative real part. We are interested in the time it takes the process to first exit the basin of attraction B of x_- starting at $x \in B$,

$$T_B(x) = \inf\{t > 0 \mid X_t \notin B\}.$$

$T_B(x)$ is a random variable, and its expectation $w_B(x) = \mathbb{E}T_B(x)$, the so-called *mean first passage time*, fulfills the inhomogeneous stationary Kolmogorov equation [15]

$$\begin{cases} \mathcal{L}w_B(x) = -1 & \text{for } x \in B \\ w_B(x) = 0 & \text{for } x \in \partial B, \end{cases} \quad (9)$$

where ∂B is the boundary of the basin of attraction of x_- , for which $\hat{n} \cdot b(u) = 0 \forall u \in \partial B$, with \hat{n} being the outwards pointing normal vector to ∂B . Here,

$$\mathcal{L} = b(x) \cdot \nabla + \frac{1}{2} \varepsilon a(x) : \nabla \nabla \quad (10)$$

is the generator of the SDE (8), from which we can deduce the invariant distribution $\rho_\infty(x)$ through the stationary Fokker-Planck equation

$$\mathcal{L}^\dagger \rho_\infty = 0,$$

where \mathcal{L}^\dagger is the L^2 -adjoint of the generator.

In the case of the gradient flow (3), the invariant distribution is given as Gibbs distribution through the potential itself,

$$\rho_\infty(x) = C e^{-U(x)/\varepsilon}. \quad (11)$$

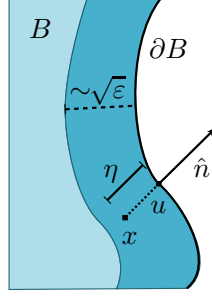


Figure 1. Schematic depiction of the boundary layer along ∂B : In an $\mathcal{O}(\sqrt{\varepsilon})$ vicinity, a point $x \in B$ is expanded along normal direction \hat{n} from boundary point $u \in \partial B$, with local coordinate $\eta > 0$.

Further, there is a distinguished point x_s on ∂B for transitions from a out of B , given through the *barrier height* [10],

$$\Delta U = \inf_{u \in \partial B} (U(u) - U(x_-))$$

i.e. the smallest potential barrier encountered by continuous curves starting at x_- and leaving through ∂B . The point at which this barrier is taken, $x_s \in \mathbb{R}^n$, must be a saddle point with a single unstable direction, i.e. $\nabla U(x_s) = 0$ and $M(x_s)\nabla\nabla U(x_s)$ having exactly one negative eigenvalue μ_- , and $n - 1$ positive eigenvalues. In general there might be multiple saddles, all of which are dominated by x_s , which is therefore called the *relevant saddle*. In the following, we write $M_s = M(x_s)$.

From large deviation theory [6] it is then known that

$$w_b(a) \asymp e^{\varepsilon^{-1}(U(s)-U(a))}, \quad (12)$$

which determines the exponential part of the mean first passage time, recovering *Arrhenius' law* [5]. The purpose of the Eyring-Kramers law, and the goal of this paper, is to go beyond this mere exponential scaling law, and get sharp asymptotics of the prefactor omitted in (12).

2.1. Asymptotic expansion and boundary layer analysis

In order to get access to the prefactor, and loosely following [15], we assume $w_B(x) \asymp e^{K/\varepsilon}$ as estimated by large deviation theory (12) and work with

$$\tau(x) = e^{-K/\varepsilon} w_B(x),$$

which fulfills, via (9), the Kolmogorov equation

$$\begin{cases} \mathcal{L}\tau(x) = -e^{-K/\varepsilon} & \text{for } x \in B \\ \tau(x) = 0 & \text{for } x \in \partial B, \end{cases}$$

so that for $\varepsilon \rightarrow 0$ the right hand side vanishes and the Kolmogorov equation becomes homogeneous. Since the diffusive term in the generator is $\mathcal{O}(\varepsilon)$ as well, we can assume that within B the variable $\tau(x)$ is merely advected and thus constant, $\tau(x) = C_0$, to leading order in ε . We need to consider only the behavior in a small $\mathcal{O}(\sqrt{\varepsilon})$ boundary layer near ∂B .

For a point x near the boundary ∂B , we choose coordinates

$$x = u - \sqrt{\varepsilon} \eta \hat{n},$$

for $\eta > 0$ and $u \in \partial B$, compare figure 1. In this boundary layer, to leading order, we therefore have

$$\mathcal{L} \approx (b(x) \cdot \hat{n}) \frac{1}{\sqrt{\varepsilon}} \partial_\eta + \underbrace{\hat{n} \cdot a(x) \hat{n}}_{\alpha(u)} \partial_\eta^2.$$

Since x is $\mathcal{O}(\sqrt{\varepsilon})$ -close to $u \in \partial B$, we can expand

$$b(x) \cdot \hat{n} = \underbrace{b(u) \cdot \hat{n}}_{=0} + \hat{n} \cdot \nabla b(u)(x - u) + \mathcal{O}(|x - u|^2),$$

and introduce the additional quantity $\beta(u)$ through

$$\hat{n} \cdot \nabla b(u)(x - u) = -\sqrt{\varepsilon} \eta \underbrace{\hat{n} \cdot \nabla b(u) \hat{n}}_{\beta(u)}.$$

We will later see that $\beta(u)$ at the saddle $u = x_s$ is related to the unstable eigenvalue μ_- . Now, all terms are $\mathcal{O}(\varepsilon^0)$ and we arrive at

$$0 = \mathcal{L}\tau(\eta) = \eta\beta(u)\partial_\eta\tau(\eta) + \alpha(u)\partial_\eta^2\tau(\eta), \quad (13)$$

with α, β being the leading-order contributions of the normal terms of a and b , respectively. Equation (13) is solved by

$$\tau(\eta) = C_1(u) \int_0^\eta e^{-\frac{\beta(u)}{2\alpha(u)}\eta^2} d\eta.$$

Since we know the limit $\tau(\eta) \xrightarrow{\eta \gg 1} C_0$, we must have the matching condition

$$C_1(u) = C_0 \sqrt{\frac{2\beta(u)}{\pi\alpha(u)}},$$

from which we can obtain C_0 . The connection between the bulk and the boundary can be exploited when integrating $\mathcal{L}\tau(x) = -e^{-K/\varepsilon}$ against the invariant density $\rho_\infty(x)$, and

integrating by parts,

$$\begin{aligned}
-e^{-K/\varepsilon} \int_B \rho_\infty(x) dx &= \int_B \rho_\infty(x) \mathcal{L}\tau(x) dx \\
&= \int_B \underbrace{(\mathcal{L}^\dagger \rho_\infty)}_{=0} \tau(x) dx + \\
&\quad \int_{\partial B} \left(\underbrace{\rho_\infty(\hat{n} \cdot b(u))}_{\tau=0 \text{ on } \partial B} \underbrace{\tau(u)}_{\tau=0 \text{ on } \partial B} + \varepsilon \left(\rho_\infty \hat{n} \cdot a(u) \nabla \tau(u) - \underbrace{\tau(u) \hat{n} \cdot a(u)}_{\tau=0 \text{ on } \partial B} \nabla \rho_\infty \right) \right) du \\
&= -\sqrt{\varepsilon} \int_{\partial B} \rho_\infty(u) \alpha(u) \partial_\eta \tau du \\
&= -\sqrt{\frac{2\varepsilon}{\pi}} C_0 \int_{\partial B} \rho_\infty(u) \sqrt{\alpha(u)\beta(u)} du
\end{aligned}$$

so that

$$C_0 = e^{-K/\varepsilon} \sqrt{\frac{\pi}{2\varepsilon}} \frac{\int_B \rho_\infty(x) dx}{\int_{\partial B} \rho_\infty(u) \sqrt{\alpha(u)\beta(u)} du}.$$

We conclude that in the interior,

$$w_B(a) = \sqrt{\frac{\pi}{2\varepsilon}} \frac{\int_B \rho_\infty(x) dx}{\int_{\partial B} \rho_\infty(u) \sqrt{\alpha(u)\beta(u)} du}. \quad (14)$$

2.2. Laplace asymptotics

Note that so far we have not made use of the gradient structure of our system, and the result (14) is asymptotically correct for $\varepsilon \ll 1$ for arbitrary systems. We can now make use of our explicit knowledge of the invariant measure (11) to apply Laplace asymptotics to the volume and boundary integrals in (14). Concretely, that means that in the numerator, we can approximate

$$\int_B \rho_\infty(x) dx \approx \frac{(2\pi\varepsilon)^{n/2}}{\sqrt{\det H_-}} e^{-U(x_-)/\varepsilon},$$

since x_- is the minimum of U within B , while in the denominator

$$\int_{\partial B} \rho_\infty(u) \sqrt{\alpha(u)\beta(u)} du \approx \frac{(2\pi\varepsilon)^{(n-1)/2}}{\sqrt{|\det H_s|}} \sqrt{\alpha(s)\beta(s)} (\hat{n} \cdot H_s^{-1} \hat{n})^{-1/2} e^{-U(x_s)/\varepsilon},$$

where the $(\hat{n} \cdot H_s^{-1} \hat{n})$ -term comes from the fact that we integrate the Gaussian integral only over the tangent space to the separatrix at the saddle, $T_{x_s} \partial B$, as derived in the appendix in lemma 4. In total, this yields

$$w_B(x_-) = \pi \sqrt{\frac{\hat{n} \cdot H_s^{-1} \hat{n}}{\alpha(x_s)\beta(x_s)}} \sqrt{\frac{|\det H_s|}{\det H_-}} e^{\Delta U/\varepsilon}$$

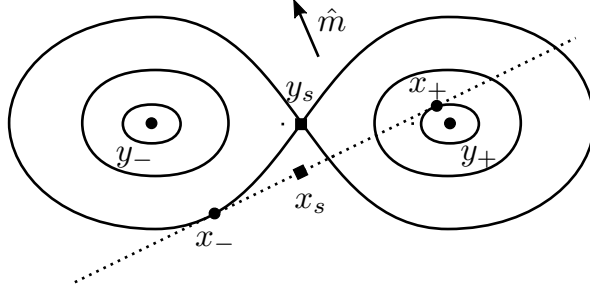


Figure 2. Conserved quantities of the stochastic process: If $M(x)$ has a zero eigenvalue with eigenvector \hat{m} , then the gradient diffusion (3) will remain constrained to a submanifold $S \in \mathbb{R}^n$ (dotted line) with normal vector \hat{m} . Instead of the actual fixpoints $\{y_-, y_s, y_+\}$, the relevant points are now the corresponding fixed points $\{x_-, x_s, x_+\}$ of the dynamics constrained to the submanifold S .

where we recall $\alpha(x_s) = \hat{n} \cdot M_s \hat{n}$ and $\beta(x_s) = \hat{n} \cdot M_s H_s \hat{n}$, and where the $\mathcal{O}(\varepsilon)$ -part of the drift term $b(x) = -M(x) \nabla U(x) + \varepsilon \nabla \cdot M(x)$ is subdominant and thus dropped.

Using lemma 2 and 3 of the appendix, we recognise that $\alpha(x_s)$ and $\beta(x_s)$ are connected to μ_- via

$$\beta(x_s) = \frac{\alpha(x_s)}{\hat{n} \cdot H_s^{-1} \hat{n}} = \mu_- ,$$

where μ_- is the unique negative eigenvalue of $M_s H_s$. We arrive at the final result

$$w_B(x_-) = \frac{\pi}{\mu_-} \sqrt{\frac{|\det H_s|}{\det H_-}} e^{\Delta U / \varepsilon} .$$

This demonstrates the capacity theory result from the literature [12] for the case of gradient flows with position-dependent mobility.

2.3. Conserved quantities of the mobility matrix

We now consider the case where the system has a conserved quantity, understood in the sense that the mobility matrix $M(x) : \mathbb{R}^n \rightarrow \mathbb{R}^{n \times n}$ is no longer positive definite, but positive semi-definite. In other words, for each $x \in \mathbb{R}^n$, there exists a number of zero eigenvalues of $M(x)$, and $M(x)$ is no longer full rank. As a consequence, since the mobility acts in front of both the deterministic drift and the stochastic noise, the degrees of freedom associated with the zero eigenvalues are never changed, and remain a constant of integration. The concrete value of the conserved quantity and their nature depends on both the mobility matrix and the initial condition of the system.

For simplicity, we consider a single conserved quantity, so that $M(x)$ has a unique zero eigenvalue for all $x \in \mathbb{R}^n$ with normalised eigenvector $\hat{m}(x)$, while all its other eigenvalues are strictly positive. The process (3) then remains constrained to an $(n-1)$ -dimensional sub-manifold $S \subset \mathbb{R}^n$, with normal vector field $\hat{m}(x)$, since neither the gradient drift nor the stochastic force can ever have a contribution in the direction of \hat{m} .

This situation is depicted in figure 2. Note that, while the original fixed points (both stable, y_{\pm} , and saddle y_s) of the system still exist, they do not lie within S . Instead, the effective stable points x_+ and x_- that should be considered for the Laplace asymptotics are no longer (local) minima of the potential $U(x)$, but instead are only local minima of the potential constrained to the submanifold S , so that $\nabla U(x_-) \parallel \hat{m}$ instead of $\nabla U(x_-) = 0$. The same is true for the effective saddle point x_s , which is no longer a proper saddle of $U(x)$. Therefore, the new basin of attraction, \tilde{B} , is now a subset of S instead of all of \mathbb{R}^n , as is its boundary, $\partial\tilde{B}$. As before, we write $M_s := M(x_s)$, $H_s = \nabla\nabla U(x_s)$ and $H_- = \nabla\nabla U(x_-)$.

In fact, all arguments made in sections 2.1 and 2.2 go through with the minor modification of operating in the $(n-1)$ -dimensional tangent spaces $T_{x_-}S$ and $T_{x_s}S$ around the stable point and the saddle instead of all of \mathbb{R}^n . This is possible in particular because at the saddle point x_s , the space of conserved quantities $T_{x_s}S$ cannot be parallel to the separatrix ∂B , or in other words $\hat{n}(x_s) \nparallel \hat{m}(x_s)$ (where we recall that $M_s\hat{m}(x_s) = 0$ and $H_s M_s \hat{n}(x_s) = \mu^+$). In fact, as shown in lemma 6, \hat{n} and \hat{m} are perpendicular in the H_s^{-1} inner product, which simplifies the integration.

A correcting factor needs to be introduced when we apply the Laplace method and integrate over $B \subset \mathbb{R}^n$ and ∂B , which are now integrals over $\tilde{B} \subset S$ and $\partial\tilde{B}$. In particular

$$\begin{aligned} \int_{\tilde{B}} f(x) e^{-U(x)/\varepsilon} dx &\stackrel{\varepsilon \rightarrow 0}{=} f(x_-) e^{-U(x_-)/\varepsilon} \int_{T_{x_-}\tilde{B}} e^{-\frac{1}{2}z \cdot H_- z} dz \\ &= \sqrt{\frac{(2\pi\varepsilon)^{n-1}}{\det H_-}} |\hat{m} \cdot H_-^{-1} \hat{m}|^{-1/2} f(x_-) e^{-U(x_-)/\varepsilon} \end{aligned}$$

at the stable fixed point, and

$$\begin{aligned} \int_{\partial\tilde{B}} f(x) e^{-U(x)/\varepsilon} dx &\stackrel{\varepsilon \rightarrow 0}{=} f(x_s) e^{-U(x_s)/\varepsilon} \int_{T_{x_s}\partial\tilde{B}} e^{-\frac{1}{2}z \cdot H_s z} d\sigma(z) \\ &= \sqrt{\frac{(2\pi\varepsilon)^{n-2}}{\det H_-}} |\hat{m} \cdot H_s^{-1} \hat{m}|^{-1/2} |\hat{n} \cdot H_s^{-1} \hat{n}|^{-1/2} f(x_s) e^{-U(x_s)/\varepsilon} \end{aligned}$$

at the saddle point, which follows from lemmas 4) and 5 in the appendix.

We thus arrive at our final result

$$\tau = \frac{\pi}{\mu_-} \sqrt{\frac{|\det H_s|}{\det H_-}} \sqrt{\frac{\hat{m} \cdot H_s^{-1} \hat{m}}{\hat{m} \cdot H_-^{-1} \hat{m}}} e^{\Delta U/\varepsilon} \quad (15)$$

Remark 1. Of course it might be simpler, in particular in finite dimensional systems, to consider instead of the original stochastic evolution equation a reduced equation that eliminates variables to enforce the conservation constraint explicitly. For example, for a chemical reaction transforming molecule A into B and back, but with the total number $A+B$ conserved, one could instead consider stochastic dynamics in the difference $A-B$. While sometimes this approach is practical, and it must lead to identical results, it often produces complicated equations, in particular in the functional setting.

2.4. Functional gradient flows and stochastic hydrodynamics

While the above discussion and derivation focuses on gradient flows in \mathbb{R}^n , following the work in [14], it has been realised that a vast array of systems that originate from macroscopic limits of microscopic interacting particle systems can similarly be interpreted as gradient flows, on the space of probability measures, and as generalised Wasserstein-gradient flows of an entropy functional. The easiest example is the many-particle limit of non-interacting Brownian walkers, in the large particle limit, $N \rightarrow \infty$, but interactions with external forces, surrounding fluids, or inter-particle interactions can be incorporated as well. For finite but large number of particles, $N \gg 1$, one expects fluctuations of the order $1/\sqrt{N}$ and arrives at a *stochastic* evolution equation in the form of a stochastic partial differential equation (SPDE), generally summarised under the notion of *fluctuating hydrodynamics* [16, 17, 18]. If the underlying microscopic model is in detailed balance, so is the resulting stochastic hydrodynamics equation. For the example of $N = 1/\varepsilon$ non-interacting random walkers,

$$dX_i(t) = \sqrt{2D}dW_i(t),$$

the limiting SPDE for the density $\rho(x, t)$ of walkers is formally given by

$$\partial_t \rho(x, t) = D\Delta \rho(x, t) + \sqrt{2D\varepsilon} \partial_x (\sqrt{\rho(x, t)} \eta(x, t)),$$

which is a functional gradient flow

$$\partial_t \rho = -M(\rho) \frac{\delta E[\rho]}{\delta \rho} + \sqrt{2\varepsilon} M_{1/2}(\rho) \eta,$$

with

$$E[\rho] = \int \rho \log \rho dx, \quad \text{and} \quad M(\rho) \xi = D \nabla \cdot (\rho \nabla \xi).$$

The above limiting equation is formal, and there is considerable effort involved in making this intuition rigorous, in particular for nonlinear equations and in higher dimensions. The precise mathematical interpretation of the resulting SPDEs is subject to active research [19, 20]. This includes, but is not limited to, the interpretation of the $\mathcal{O}(\varepsilon)$ -divergence term in (3), which for many nonlinear equations diverges and requires renormalization. For the purposes of this paper, we retreat to the notion that ultimately, every numerical computation relies on discretization and hence an “UV” cutoff that regularises any divergences. In systems of physical meaning, such a cut-off can be naturally justified as length scale where the continuum limit breaks down, such as the size of a molecule for a fluid. In this sense, any spatially continuous SPDE is to be interpreted as a notational shorthand for a discrete system with an appropriate physical cut-off length scale.

2.5. Full computational scheme

Given the above derivation, we now have a complete recipe for computing mean first passage times for metastable stochastic hydrodynamics. Concretely, in order to estimate

the mean first passage time out of a locally stable configuration, we apply the following steps:

- (i) Compute the saddle point (for example via edge tracking or gentlest ascent dynamics (GAD) [21]) constrained to the submanifold restriction, respecting the conserved quantities.
- (ii) Compute the Hessian around the effective saddle and stable fixed point by discretizing the continuous operator via some spatial discretization scheme.
- (iii) Compute the spectrum of this Hessian, and correct for its action in conserved normal direction (the subspace perpendicular to mass conservation).

The result will be a quantitative estimate for the mean first passage time for the small noise limit. Notably, there is no fitting parameter or additional assumption. The computation has to be done only once, and can then be used for any noise strength ε (but of course will be more accurate for smaller ε).

In the following section, we will demonstrate the applicability of this scheme to a number of examples, starting with a two-dimensional and easy to visualise toy example in section 3, and then two stochastic partial differential equations motivated from interacting particle systems and stochastic hydrodynamics: the rupture time for liquid thin films in section 4, and the a socio-economic model of urban separation in section 5.

3. Two-dimensional gradient flow

As a simple and easy to visualise example, we first consider a double-well for $(x, y) \in \mathbb{R}^2$ given by

$$U(x, y) = \frac{1}{4}(1 - x^2)^2 + \frac{1}{2}y^2(x^2 + \frac{1}{4}). \quad (16)$$

While this potential has two minima, at $(-1, 0)$ and $(1, 0)$, and a saddle at $(0, 0)$, we want to modify the gradient flow with the mobility matrix

$$M(x, y) = \frac{1}{2}(1 + x^2)\hat{p}\hat{p}^T,$$

for a normalised vector $\hat{p} \in \mathbb{R}^2$. Since $M(x)$ has a zero eigenvalue with corresponding eigenvector $\hat{m} = (\hat{p})^\perp$, the gradient flow

$$d(X_t, Y_t) = -M(X_t, Y_t)\nabla U(X_t, Y_t) dt + \sqrt{2\varepsilon}M^{1/2}(X_t, Y_t) (dW_x, dW_y) \quad (17)$$

will always remain confined to the subspace

$$S = \{(x, y) \in \mathbb{R}^2 \mid (x, y) \cdot \hat{m} = k\}.$$

In other words, the quantity $k = (x, y) \cdot \hat{m}$ is a conserved quantity of equation (17), similar to how mass is conserved in fluctuating hydrodynamic equations. Its value throughout remains that of the initial conditions of (17). This situation is depicted in figure 3 (left).

For a numerical experiment to demonstrate the correctness of our formula, we concretely pick $p = (1, \frac{1}{4})$ and $\hat{p} = p/|p|$, and initialise with the conserved quantity set

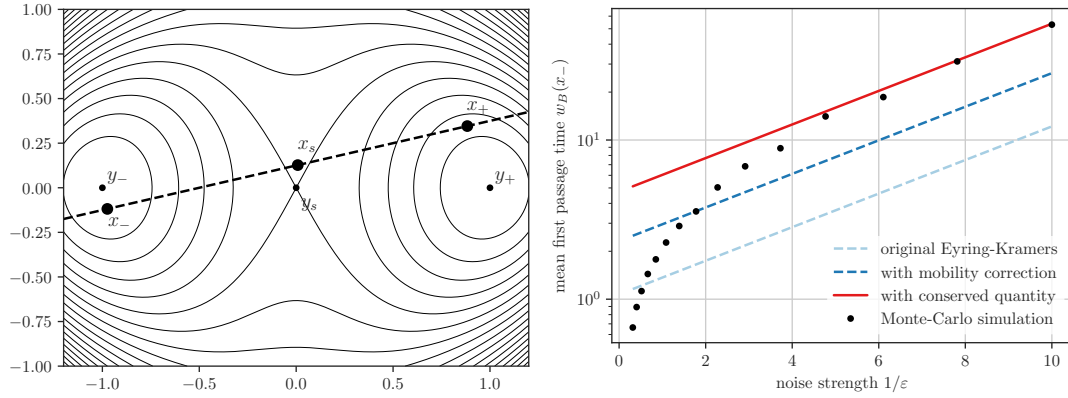


Figure 3. Left: Doublewell (16) with conserved quantity. While the full double-well, with minima y_{\pm} and saddle y_s , adheres to the original Eyring-Kramers formula (4), the actual system (17) has a conserved quantity, restricting it to the dashed subspace. Not only does this result in different minima x_{\pm} and saddle x_s of the restricted system, but the ratio of Hessians in the Eyring-Kramers formula becomes incorrect, as it considers curvatures into suppressed directions. **Right:** Time to leave the basin of attraction of x_- as a function of the noise amplitude ε . Dots show the result of 1000 numerical simulations of (17) each, compared to the original Eyring-Kramers formula (2) (light blue dashed), the formula (4) taking into account the mobility matrix (dark blue dashed), and finally our formula (15) further taking into account the conserved quantities (red solid). Clearly, both corrections are needed to explain the observed times.

to $k = \frac{1}{8}$. With these values, we can numerically measure the mean time it takes to exit the basin of attraction of the left well, and compare the results to our formula in section 2. The equation 17 is solved using a fourth order Runge-Kutta method [22] with timestep $dt = 5 \cdot 10^{-3}$. Figure 3 (right) shows the results of the Monte-Carlo experiment, simulating $N = 1000$ samples for each value of ε and averaging the observed time to exit the basin of attraction of the left well. This is compared against the original Eyring-Kramers formula (2) considering only the properties of the Hessian (light blue dashed), the generalised Eyring-Kramers formula including the correction from the mobility operator, equation (4) (dark blue dashed), and lastly our final result (15) which further considers the correction of the restriction to the conserved subspace. As can be seen, the change of eigenvalue from λ_- to μ_- , as well as the conserved quantity correcting factor $\sqrt{(\hat{m} \cdot H_s^{-1} \hat{m}) / (\hat{m} \cdot H_-^{-1} \hat{m})}$, both lead to a correcting factor of roughly 2, and both corrections are needed in order to explain the observed result. We stress that in order to obtain the fully corrected Eyring-Kramers law (15), a single computation needs to be done for a prediction for all ε , and without any fitting parameter. The small noise limit, $\varepsilon \ll 1$, appears to work reasonably well already for values $\varepsilon < \frac{1}{4}$.

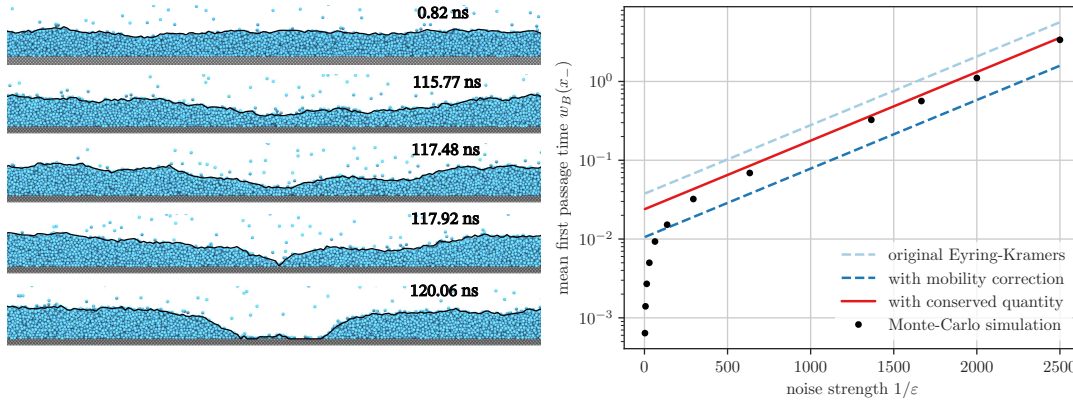


Figure 4. **Left:** Snapshots from molecular dynamics simulation of a thin liquid film on a solid substrate. The blue particles indicate liquid and vapor. The silver particles indicate solid. The black lines show the position of the liquid-vapor interface, i.e. the film height. While the film is initially flat, it eventually ruptures by thermal fluctuations. **Right:** Average waiting time for rupture of thin film is plotted as a function of the inverse strength of the fluctuations. As ϵ decreases, the observed average rupture time collapse onto the Eyring-Kramers prediction with our expression for the prefactor (15).

4. Stochastic Hydrodynamics and Thin Film Rupture

The stability of nanoscale thin liquid films on solid substrates plays a key role in many applications including coating [23], nanofluidic transistors [24] and nanomanufacturing [25]. It has been observed both experimentally [26, 27, 28] and numerically with molecular dynamics simulations [29, 30, 31] that initially flat films would rupture spontaneously, as shown in figure 4 (left). The classical explanation for the rupture is due to the competition between the disjoining pressure (otherwise known as the van der Waals forces) and the surface tension, and a linear stability analysis [32] further reveals a critical wavelength above which the wave modes are linearly unstable, eventually leading to rupture. However, subsequent observations [28] have revealed a larger set of regimes, one of which was hypothesised to stem from *thermally* activated rupture in the linearly stable regime.

Nanoscale films are difficult to observe experimentally and often molecular dynamics is utilised to explore their stability. However, MD can be computationally expensive, and thus there has been a drive towards developing macroscopic models to model this system. It has been observed [33, 34] that the evolution of the thin film follows a stochastic hydrodynamic limit, namely the stochastic thin film equation (STF) which, in the two-dimensional case, after non-dimensionalisation [31] reads

$$\partial_t h(x, t) = \partial_x \left[c(h) \partial_x \left(-\partial_x^2 h + \frac{4\pi^2}{3h^3} \right) + \sqrt{2\epsilon c(h)} \eta \right]. \quad (18)$$

Here, $h(x, t)$ is the height of the thin film, $c(h) = h^3$ is the mobility associated with a no-slip solid, ϵ is the noise amplitude and η is a Gaussian white noise uncorrelated in

both time and space, i.e. $\langle \eta(x, t) \eta(x', t') \rangle = \delta(x - x') \delta(t - t')$ where $\langle \cdot \rangle$ is the ensemble average and $\delta(x)$ is the Dirac delta functional. The STF is assumed to be periodic on $x \in [0, 1]$ and the non-dimensionalisation is chosen so that the linear stability depends solely on the average film height $h_0 = \int_0^1 h(x, t) dx = \text{const}$: for $h_0 > 1$ the film is linearly stable and small perturbations without thermal fluctuations would decrease exponentially with time. For simplicity we use a constant mobility $c(h) = h_0^3$. The STF can also be interpreted as a functional gradient flow

$$\partial_t h(x, t) = -M(h) \frac{\delta E}{\delta h} + \sqrt{2\varepsilon} M_{1/2}(h) \eta,$$

for an energy functional

$$E[h] = \int_0^1 \left(\frac{1}{2} (\partial_x h)^2 - \frac{2\pi^2}{3h^2} \right) dx, \quad (19)$$

with mobility operator

$$M(h) \circ = -\partial_x (h_0^3 \partial_x \circ),$$

and

$$M_{1/2}(h) \circ = \sqrt{h_0^3} \partial_x \circ.$$

The thermally activated rupture of the liquid nanofilm can then be interpreted as a diffusive exit of the SPDE (18) from the basin of attraction of the spatially constant solution

$$h(x, t) = h_0 > 1.$$

Additionally, the system obeys mass conservation, and as such constant functions are a zeromode of the mobility operator. Therefore, in order to compute the expected time to rupture, our full formalism (15) is necessary. Specifically, the computation consists of the following steps: (1) We compute the saddle point of the energy functional (19) via GAD, (2) we compute the second variation of the energy functional, acting on a test function $\xi(x)$ at an arbitrary point h^* , given by (see Appendix B)

$$\left. \frac{\delta^2 E[h(x)]}{\delta h(x)^2} \right|_{h=h^*} \circ \xi(x) = -\frac{4\pi^2}{h^*(x)^4} \xi(x) - \partial_x^2 \xi(x),$$

and compute numerically the spectrum of this operator at the fixed point, $h^* = h_0$, and at the saddle, $h^* = h_s(x)$. The ratio of these Hessians, evaluated according to equation (2), yields the light blue dashed line in figure 4. (3) Since the mobility operator is not the identity, there is a correcting factor including μ_- , which we obtain numerically by computing the unique negative eigenvalue of the operator

$$M(h_s(x)) \frac{\delta^2 E[h]}{\delta h^2} \Big|_{h=h_s} \circ = h_0^3 \partial_x^2 \left[\left(\frac{4\pi^2}{h_s(x)^4} + \partial_x^2 \right) \circ \right],$$

which yields instead the dark blue dashed line in figure 4. Lastly, we need to compute the action of the Hessian in direction of the vector normal to the conserved submanifold,

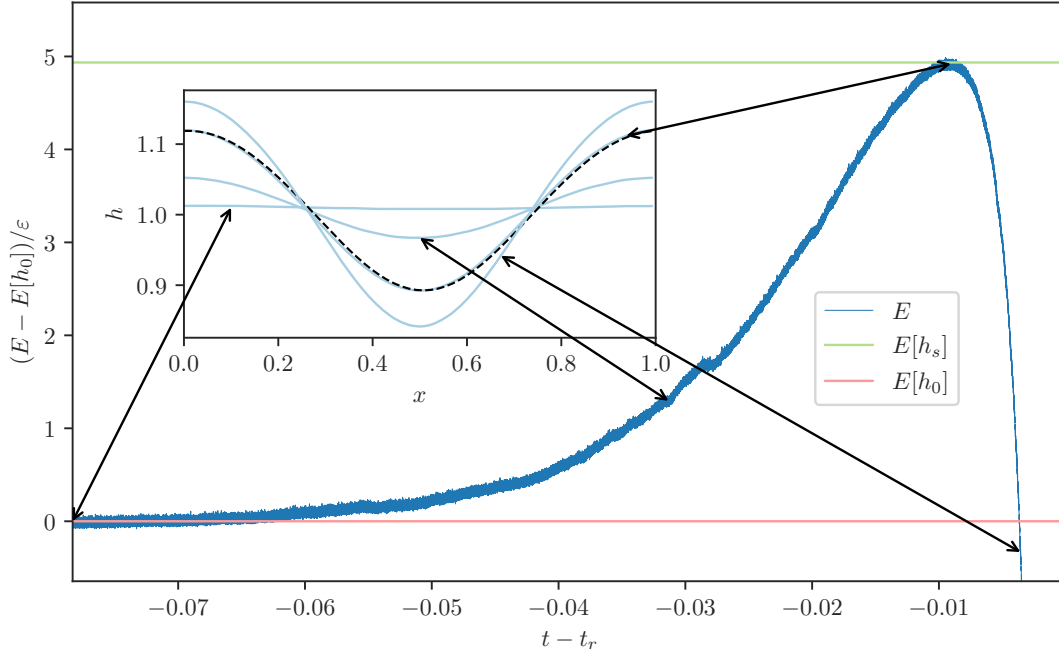


Figure 5. Change of energy near rupture time. Noise amplitude is chosen to be $\varepsilon = 0.0005$. The dark blue line is the energy of the averaged profile, the light red line is the energy of the flat profile and the light green line is the energy of the saddle shape calculated analytically via GAD. The energy is translated by the energy of the flat profile and normalised by noise amplitude ε . The inset shows the averaged profile at different times with light blue lines and the analytical saddle shape with black dashed lines.

which in this case is just the constant function $1(x) \equiv 1$. The inverse of the Hessian operator is evaluated numerically, and the result is the red solid line in figure 4, which agrees very well with the waiting time to rupture obtained via many stochastic Monte-Carlo experiments that integrate the stochastic thin film equation (18) until a rupture is observed (black dots). The exponential time differencing method (ETD) [35] is used for the Monte-Carlo experiments with timestep $dt = 1.566 \cdot 10^{-7}$, and the details of implementation can be found in [31]. Here we choose the average film height to be $h_0 = 1.01$, the STF is solved on a domain with 128 uniformly distributed grid points, and the rupture times are averaged over 100 events. Note that in [31], additional molecular dynamics simulations demonstrated agreement of expected rupture times with equation (15).

To further characterise the rupture process, we investigate how the energy (19) changes with time near rupture. We perform 200 independent simulations and record the film profiles for $5 \cdot 10^5$ timesteps before the rupture time t_r . The energy is then calculated with the averaged profile to filter out the effect of thermal fluctuations, as shown in figure 5. The light blue lines and the black dashed line in the inset show the averaged profiles at different times and the analytical saddle shape calculated from GAD, respectively. It is shown that the energy increase as the averaged profile deviates

from its flat steady state, until the averaged profile reaches the saddle shape h_s and drops dramatically. The analytical energy barrier is recovered from the simulations, and the analytical saddle shape agrees well with the averaged profile with maximum energy. These findings indicate that our saddle shape calculation is correct and the transition (or rupture) indeed goes through the saddle.

5. Social dynamics and urban segregation

Fluctuating hydrodynamics SPDEs are not only encountered in continuum limits of actual fluid models, but are regularly derived whenever there is a large number of interacting agents, such as interacting active particles [36], in traffic flow [37], pedestrian dynamics [38, 39] and socioeconomic interactions [40]. In each case, the particles are replaced by agents capable of acting according to some simple ruleset. In socioeconomic models, a generic assumption is that the agents try to individualistically improve their own outcome or utility. In this context, the number of possible equilibrium states of the overall model, as well as their relative likelihood, becomes extremely important, as it describes directly the most likely emergent state that the system will spontaneously converge to. Consequently, the convergence to the ultimate stable state can be seen as the manifestation of the “invisible hand” crystallizing the collective societal state out of the individual agents’ behavior.

A well-known example is the phenomenon of urban segregation, described by the Schelling or Sakoda-Schelling models [41, 42]. In these, a large number of agents is prescribed, each belonging to one of multiple distinct sub-populations, for example representing social or ethnic background, which are free to relocate depending on their preferences. In the original model, the presence of only a slight preference of agents to surround themselves with neighbors of their own sub-population led to completely segregated geographical regions in the long-time limit. Following ideas introduced in [43, 44, 40], these models can be simplified to consist only of a single population, with spatial exclusion and density dependent diffusivity, leading to a fluctuating hydrodynamic equation of

$$\partial_t \rho = \nabla \cdot ((1 - \rho) \nabla (D(\rho) \rho) + \rho D(\rho) \nabla \rho) + \nabla \cdot (\sqrt{\rho(1 - \rho)} \eta(x, t)), \quad (20)$$

where η is spatio-temporally white noise and the diffusivity of agents is given by

$$D(\rho) = D_0 e^{-CK \star \rho}. \quad (21)$$

This diffusivity exhibits a spatial convolution “ \star ” with a kernel K , representing non-local sensing of their neighborhood by each of the agents. In essence, equation (20) describes the (nonlinear) diffusion of agents under spatial exclusion, such that the density remains between 0 and 1, representing complete absence of agents to full occupation. The density dependent diffusivity (21) represents the tendency of agents to relocate towards a higher density of peers in the vicinity, up to some maximum range given by a spatial cutoff of

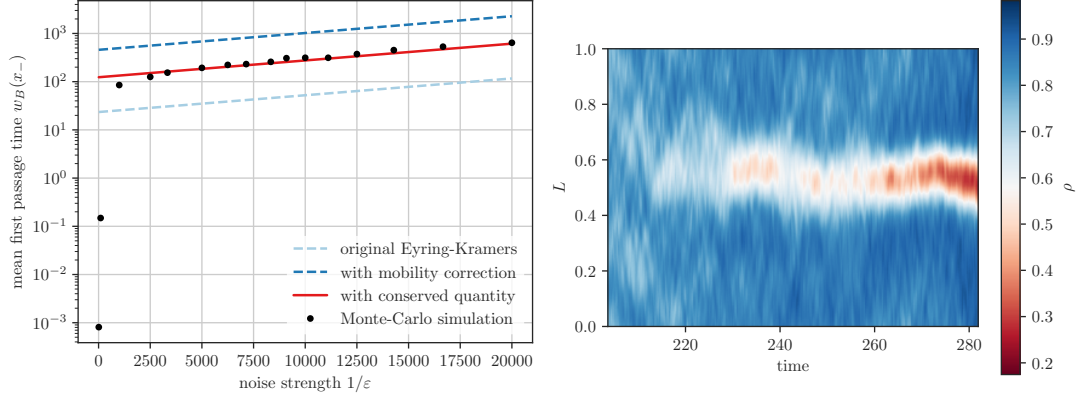


Figure 6. Left: Average waiting time for the spontaneous segregation of the social dynamics model as a function of the inverse strength of fluctuations. After a transient for large noise, waiting times are exponentially distributed. The correct exponential distribution is correctly predicted, including its prefactor, by our formula (15), while naive application of the Eyring-Kramers formula leads to mispredictions of a factor 5. **Right:** Evolution (time-space) of the density of agents near an observed segregation event. The originally homogeneous and fluctuating distribution of agents spontaneously segregates into a dense and a diluted region.

the (symmetric) kernel $K(x, y) = K(x - y)$. This corresponds to energy and mobility given by

$$\begin{cases} E[\rho] = \int (\rho \log \rho + (1 - \rho) \log(1 - \rho) - \frac{1}{2} C \rho K \star \rho) dx \\ M(\rho) \circ = -\nabla \cdot (\rho(1 - \rho) D(\rho) \nabla \circ), \\ M_{1/2}(\rho) \circ = \nabla \cdot (\sqrt{\rho(1 - \rho)} D(\rho) \nabla \circ), \end{cases} \quad (22)$$

where the mobility again conserves total mass, and we are in the framework where our results apply.

For simplicity, we assume the population density ρ is periodic on domain $x \in [0, 1]$. We also assume a Gaussian kernel $K(z) = \frac{1}{\sqrt{2\pi\kappa}} \exp(-\frac{1}{2}z^2/\kappa^2)$ with sensing length scale $\kappa > 0$, corresponding to $\hat{K}(k) = \exp(-k^2\kappa^2/2)$ in Fourier space. Expanding the convolution for $\kappa \ll 1$ yields (see Appendix C)

$$(K \star \rho)(x) = \rho(x) + \frac{\kappa^2}{2} \partial_x^2 \rho(x) + \mathcal{O}(\kappa^4).$$

The Hessian operating on a periodic test function $\xi(x)$ can then be expressed by (see Appendix B)

$$\frac{\delta^2 E[\rho(x)]}{\delta \rho(x)^2} \circ \xi(x) = \left(\frac{1}{\rho(x)} + \frac{1}{1 - \rho(x)} - C \right) \xi(x) - \frac{\kappa^2}{2} C \partial_x^2 \xi(x).$$

For simplicity, we further assume that the population density is constant in the mobility operator, $\rho(x) = \bar{\rho}$, where $\bar{\rho} = \int_0^1 \rho dx$ is the mass that is conserved. We can then calculate μ_- by numerically computing the unique negative eigenvalue of the operator

$$M(\bar{\rho}) \frac{\delta^2 E[\rho]}{\delta \rho^2} \circ = -\bar{\rho}(1 - \bar{\rho}) D(\bar{\rho}) \partial_x^2 \left[\left(\frac{1}{\bar{\rho}} + \frac{1}{1 - \bar{\rho}} - C - \frac{\kappa^2}{2} C \partial_x^2 \right) \circ \right].$$

For the parameter $C = 6$, $\kappa = 8 \cdot 10^{-3}$, $D_0 = 1$ and mass $\bar{\rho} = \int \rho dx = 0.7908$, this system exhibits multiple stable fixed points: A spatially homogeneous solution $\rho(x) = \bar{\rho}$, as well as a localised (“cluster” or “aggregated”) state with minimum $\rho_{min} = 0.1747$, which observes an aggregation of the agents in part of the domain, leaving behind a depleted region where the concentration of agents is low. Both of these states are locally stable and hence long lived for small enough fluctuations. Fluctuations are understood to be spontaneous local movements of agents, preserving their total number, but rearranging them locally in space, with probabilities based both on the local densities (through the exclusion terms proportional to $\rho(1 - \rho)$, which prevents movement out of empty or into fully occupied regions), as well as their perceived relative attractiveness encoded in the energy functional. As a result, an initially homogeneous population will eventually spontaneously segregate due to fluctuations. Population density ρ is discretised with 64 uniformly distributed grid points. Equation (20) is solved numerically using the same exponential time difference scheme as in the previous section with timestep $dt = 7.832 \cdot 10^{-5}$. The population density is segregated when its minimum has reached ρ_{min} , and we record the waiting times averaged over 100 realisations for different noise amplitude ε . These waiting times have an exponential distribution, correctly predicted by our formula (15), as shown in figure 6 (left, red line), while using the original Eyring-Kramers formula, or the mobility correction only leads to mispredictions by a factor approximately 5.

Figure 6 (right) shows a single segregation event, in which an initially homogeneous population of agents is driven to segregation by fluctuations that locally deplete the population strong enough for a gap to form, transitioning into the segregated state with a dilute region and an aggregate.

6. Conclusion

We show how recent breakthroughs in the derivation of mean first passage times to leave the basin of attraction of metastable states can be generalised to compute expected waiting times for wide classes of (generalised) gradient flows in the presence of conserved quantities. These generalizations are particularly important when applied to fluctuating hydrodynamics equations, which are limiting equations of interacting particle systems in the limit of many particles.

Such equations are ubiquitous in nature, whenever a large number of interacting agents leads to complex emergent behavior: Apart from molecular dynamics and its applications in chemistry and material design, systems such as traffic flows, pedestrian dynamics, or socioeconomics must follow similar large-scale limits. All these systems usually possess conserved quantities, such as mass or number-of-agents, energy, or momentum, which lead to divergences in the naive application of the limiting equations for mean first passage times due to zero-eigenvectors in the corresponding mobility operator.

Here, we show how we can generalise existing results to incorporate (1) position

dependent mobility, (2) degenerate mobility operators including zero-modes, (3) formally the functional setting, where we are applying our results successfully to gradient flows in function spaces. The result is a closed formula for the expected passage times for leaving a locally stable basin of attraction of the stochastic dynamics in the low-noise limit. We demonstrate our results to be applicable in a broad class of settings, including liquid nanofilm rupture times as well as social dynamics with urban segregation. The results are very generally applicable to other systems of the same class, including shallow water flows, Elo dynamics, or traffic flows.

Acknowledgments

TG would like to thank A. Donev for interesting discussions. TG acknowledges the support received from the EPSRC projects EP/T011866/1 and EP/V013319/1. JES acknowledges the support from EPSRC grants EP/W031426/1, EP/S029966/1 and EP/P031684/1. JBL was supported by a studentship within the EPSRC-supported Centre for Doctoral Training in modeling of Heterogeneous Systems, Grant No. EP/S022848/1. Relevant code used in this paper is openly available at: https://github.com/JingBang-Liu/fluctuating_hydrodynamics_first_passage_time.

References

- [1] Brinkman B A W, Yan H, Maffei A, Park I M, Fontanini A, Wang J and La Camera G 2022 *Applied Physics Reviews* **9** 011313
- [2] Ashwin P and von der Heydt A S 2020 *Journal of Statistical Physics* **179** 1531–1552
- [3] Lohmann J, Dijkstra H A, Jochum M, Lucarini V and Ditlevsen P D 2024 *Science Advances* **10** eadi4253
- [4] Bashkirtseva I and Ryashko L 2011 *Chaos: An Interdisciplinary Journal of Nonlinear Science* **21** 047514
- [5] Arrhenius S 1889 *Zeitschrift fuer physikalische Chemie* **4** 226–248
- [6] Freidlin M I and Wentzell A D 2012 *Random perturbations of dynamical systems* vol 260 (Springer)
- [7] Eyring H 1935 *The Journal of Chemical Physics* **3** 107–115
- [8] Kramers H A 1940 *Physica* **7** 284–304
- [9] Bovier A, Eckhoff M, Gaynard V and Klein M 2004 *Journal of the European Mathematical Society* **6** 399–424
- [10] Berglund N 2013 *Markov Processes and Related Fields* **19** 459–490
- [11] Bouchet F and Reygner J 2016 *Annales Henri Poincaré* **17** 3499–3532
- [12] Landim C and Seo I 2018 *Communications on Pure and Applied Mathematics* **71** 203–266
- [13] Landim C, Mariani M and Seo I 2019 *Archive for Rational Mechanics and Analysis* **231** 887–938
- [14] Jordan R, Kinderlehrer D and Otto F 2006 *SIAM Journal on Mathematical Analysis*
- [15] Gardiner C 2009 *Stochastic Methods: A Handbook for the Natural and Social Sciences* (Springer)
- [16] Bedeaux D and Mazur P 1974 *Physica* **76** 247–258
- [17] Dean D S 1996 *Journal of Physics A: Mathematical and General* **29** L613
- [18] Landau L D and Lifshitz E M 2007 *Lehrbuch der theoretischen Physik VI - Hydrodynamik* 5th ed (Verlag Harri Deutsch)
- [19] Fehrman B and Gess B 2023 *Inventiones mathematicae* **234** 573–636
- [20] Djurdjevac A, Kremp H and Perkowski N 2024 *Stochastics and Partial Differential Equations: Analysis and Computations*

- [21] E W and Zhou X 2011 *Nonlinearity* **24** 1831
- [22] Kasdin N J 1995 *Journal of Guidance, Control, and Dynamics* **18** 114–120
- [23] Weinstein S J and Ruschak K J 2004 *Annual Review of Fluid Mechanics* **36** 29–53
- [24] Karnik R, Fan R, Yue M, Li D, Yang P and Majumdar A 2005 *Nano Letters* **5** 943–948
- [25] Makarov S V, Milichko V A, Mukhin I S, Shishkin I I, Zuev D A, Mozharov A M, Krasnok A E and Belov P A 2016 *Laser & Photonics Reviews* **10** 91–99
- [26] Herminghaus S, Jacobs K, Mecke K, Bischof J, Fery A, Ibn-Elhaj M and Schlagowski S 1998 *Science* **282** 916–919
- [27] Xie R, Karim A, Douglas J F, Han C C and Weiss R A 1998 *Physical Review Letters* **81** 1251–1254
- [28] Seemann R, Herminghaus S and Jacobs K 2001 *Physical Review Letters* **86** 5534–5537
- [29] Nguyen T D, Fuentes-Cabrera M, Fowlkes J D and Rack P D 2014 *Physical Review E* **89** 032403
- [30] Zhang Y, Sprittles J E and Lockerby D A 2019 *Physical Review E* **100** 023108
- [31] Sprittles J E, Liu J, Lockerby D A and Grafke T 2023 *Physical Review Fluids* **8** L092001
- [32] Ruckenstein E and Jain R K 1974 *Journal of the Chemical Society, Faraday Transactions 2* **70** 132
- [33] Grün G, Mecke K and Rauscher M 2006 *Journal of Statistical Physics* **122** 1261–1291
- [34] Durán-Olivencia M A, Gvalani R S, Kalliadasis S and Pavliotis G A 2019 *Journal of Statistical Physics* **174** 579–604
- [35] Cox S and Matthews P 2002 *Journal of Computational Physics* **176** 430–455
- [36] Manacorda A and Puglisi A 2017 *Phys. Rev. Lett.* **119**(20) 208003
- [37] Chu K C, Yang L, Saigal R and Saitou K 2011 Validation of stochastic traffic flow model with microscopic traffic simulation *2011 IEEE International Conference on Automation Science and Engineering* pp 672–677
- [38] Carrillo J A, Martin S and Wolfram M T 2016 *Mathematical Models and Methods in Applied Sciences* **26** 671–697
- [39] Aurell A and Djehiche B 2019 *Transportation Research Part B: Methodological* **121** 168–183
- [40] Zakine R, Garnier-Brun J, Becharat A C and Benzaquen M 2024 *Phys. Rev. E* **109**(4) 044310
- [41] Schelling T C 1971 *The Journal of Mathematical Sociology* **1** 143–186
- [42] Sakoda J M 1971 *The Journal of Mathematical Sociology* **1** 119–132
- [43] Grauwin S, Bertin E, Lemoy R and Jensen P 2009 *Proceedings of the National Academy of Sciences* **106** 20622–20626
- [44] Burger M, Pietschmann J F, Ranetbauer H, Schmeiser C and Wolfram M T 2022 *European Journal of Applied Mathematics* **33** 111–132
- [45] Parr R G and Weitao Y 1995 *Density-Functional Theory of Atoms and Molecules* (Oxford University Press)

Appendix A.

Lemma 1. *Let s be the relevant saddle, and μ_- the unique unstable eigenvector of $M_s H_s$, and \hat{n} the normal vector to ∂B at the saddle. Then*

$$H_s M_s \hat{n} = \mu_- \hat{n}, \quad (\text{A.1})$$

i.e. \hat{n} is an eigenvector of $H_s M_s$ with eigenvalue μ_- .

Proof. Let $V^+ = T_{x_s} \partial B$ be the tangent space to the separatrix at the saddle, which is spanned by the $n-1$ eigenvectors $\{v_i^+\}_{i \in \{1, \dots, n-1\}}$ that correspond to positive eigenvalues μ_i^+ of $M_s H_s$. All these stable eigenvectors are parallel to the separatrix, implying $v_i^+ \cdot \hat{n} = 0$ for all i . Further, denote by v^- the unique unstable eigenvector of $M_s H_s$ with

eigenvalue μ_- . Together, the v_i^+ and v^- span all of \mathbb{R}^n and we can write every vector $v \in \mathbb{R}^n$ as

$$v = c^- v^- + \sum_i c_i^+ v_i^+ \quad \text{with} \quad c^-, c_1^+, \dots, c_{n-1}^+ \in \mathbb{R}. \quad (\text{A.2})$$

Then

$$\begin{aligned} \hat{n} \cdot M_s H_s v &= c^- \hat{n} \cdot M_s H_s v^- + \sum_i c_i^+ \hat{n} \cdot M_s H_s v_i^+ \\ &= \mu_- c^- \hat{n} \cdot v^- + \sum_i c_i^+ \mu_i^+ \underbrace{\hat{n} \cdot v_i^+}_{=0} \\ &= \mu_- \left(c^- v^- \cdot \hat{n} + \sum_i c_i^+ \underbrace{v_i^+ \cdot \hat{n}}_{=0} \right) = \mu_- v \cdot \hat{n}. \end{aligned}$$

We conclude

$$v \cdot H_s M_s \hat{n} = \mu_- v \cdot \hat{n}. \quad (\text{A.3})$$

Since (A.3) holds for arbitrary v , we obtain the statement (A.1). \square

Lemma 2. *At the saddle, $x = x_s$,*

$$\beta(x_s) = \hat{n} \cdot M_s H_s \hat{n} = \mu_-. \quad (\text{A.4})$$

Proof. Follows immediately from lemma 1. \square

Lemma 3. *At the saddle, $x = x_s$,*

$$\mu_- = \frac{\alpha(s)}{\hat{n} \cdot H_s^{-1} \hat{n}}. \quad (\text{A.5})$$

Proof. For $\alpha(s) = \hat{n} \cdot M_s \hat{n}$, we have

$$M_s \hat{n} = \mu_- H_s^{-1} \hat{n} \quad (\text{A.6})$$

from lemma 1. Solving for μ_- yields

$$\mu_- = \frac{\hat{n} \cdot M_s \hat{n}}{\hat{n} \cdot H_s^{-1} \hat{n}} = \frac{\alpha(s)}{\hat{n} \cdot H_s^{-1} \hat{n}}, \quad (\text{A.7})$$

which is the desired result. \square

Lemma 4. *Let N be a co-dimension 1 hyperplane in \mathbb{R}^n with normal vector \hat{n} , and $H \in \mathbb{R}^{n \times n}$ positive definite. Then, the Gaussian integral, restricted to the hyperplane N , is given by*

$$\int_N e^{-\frac{1}{2} y \cdot H y} d\sigma(y) = (2\pi)^{(n-1)/2} |\hat{n} \cdot H^{-1} \hat{n}|^{-1/2} |\det H|^{-1/2}. \quad (\text{A.8})$$

Proof. We have

$$\int_{\mathbb{R}^n} e^{-\frac{1}{2}z \cdot Hz} dz = (2\pi)^{n/2} |\det H|^{-1/2}. \quad (\text{A.9})$$

In order to obtain a formula for the restricted Gaussian integral, consider the coordinate change

$$z = y + sH^{-1}\hat{n} \quad \text{with} \quad y \in N, \quad s \in \mathbb{R}. \quad (\text{A.10})$$

Since we can write $H^{-1}\hat{n} = (\hat{n} \cdot H^{-1}\hat{n})\hat{n} + v$, where $v \in N$, we know that the change of variables yields

$$dz = d(H^{-1}\hat{n}) \wedge dy = |\hat{n} \cdot H^{-1}\hat{n}| d\sigma(y) ds. \quad (\text{A.11})$$

Thus,

$$\begin{aligned} \int_{\mathbb{R}^n} e^{-\frac{1}{2}z \cdot Hz} dz &= |\hat{n} \cdot H^{-1}\hat{n}| \int_{\mathbb{R}} \int_N e^{-\frac{1}{2}(y+sH^{-1}\hat{n}) \cdot H(y+sH^{-1}\hat{n})} d\sigma(y) ds \\ &= |\hat{n} \cdot H^{-1}\hat{n}| \left(\int_N e^{-\frac{1}{2}y \cdot Hy} d\sigma(y) \right) \left(\int_{\mathbb{R}} e^{-\frac{1}{2}s^2(\hat{n} \cdot H^{-1}\hat{n})} ds \right) \\ &= (2\pi)^{1/2} |\hat{n} \cdot H^{-1}\hat{n}|^{1/2} \int_N e^{-\frac{1}{2}y \cdot Hy} d\sigma(y), \end{aligned}$$

and via equation (A.9) we arrive at the desired result. \square

Lemma 5. *Let N and M be two co-dimension 1 hyperplanes in \mathbb{R}^n with normal vectors \hat{n} and \hat{m} , respectively, and $H \in \mathbb{R}^{n \times n}$ positive definite. Then, the Gaussian integral, restricted to the intersection of the two hyperplanes $N \cap M$, is given by*

$$\int_{N \cap M} e^{-\frac{1}{2}x \cdot Hx} dx = (2\pi)^{(n-2)/2} |\hat{n} \cdot H^{-1}\hat{n}|^{1/2} |\hat{m} \cdot H^{-1}\hat{m}|^{1/2} (\det H)^{1/2} \quad (\text{A.12})$$

if \hat{n} and \hat{m} are orthogonal in the H^{-1} inner product,

$$\hat{n} \cdot H^{-1}\hat{m} = 0. \quad (\text{A.13})$$

Proof. With a similar argument as before, consider the coordinate change

$$z = y + sH^{-1}\hat{n} + tH^{-1}\hat{m} \quad \text{with} \quad y \in N \cap M, \quad s, t \in \mathbb{R} \quad (\text{A.14})$$

Then, the volume element yields

$$dz = dy \wedge d(H^{-1}\hat{n}) \wedge d(H^{-1}\hat{m}) = |(\hat{n} \cdot H^{-1}\hat{n})(\hat{m} \cdot H^{-1}\hat{m}) - (\hat{n} \cdot H^{-1}\hat{m})(\hat{m} \cdot H^{-1}\hat{n})| d\sigma(y) ds dt. \quad (\text{A.15})$$

Since by assumption $\hat{n} \cdot H^{-1}\hat{m} = \hat{m} \cdot H^{-1}\hat{n} = 0$, we arrive at the desired result with the same in lemma 4. \square

Lemma 6. *Let \hat{m} be the zero eigenvector of the mobility matrix $M(x_s)$ at the saddle x_s , and \hat{n} the normal vector to the separatrix ∂B at the saddle x_s . Then*

$$\hat{n} \cdot H_s^{-1}\hat{m} = \hat{m} \cdot H_s^{-1}\hat{n} = 0. \quad (\text{A.16})$$

Proof. From lemma 1 we know

$$M_s \hat{n} = \mu_- H_s^{-1} \hat{n}, \quad (\text{A.17})$$

and thus

$$\hat{m} \cdot H_s^{-1} \hat{n} = \frac{1}{\mu_-} \hat{m} \cdot M \hat{n} = \frac{1}{\mu_-} \hat{n} \cdot M \hat{m} = 0. \quad (\text{A.18})$$

□

Appendix B. Hessian as second variation

In this section we sketch a formal derivation of Hessian of a given energy functional. We first show the derivation of the Hessian of the energy functional of the STF. The functional derivative of the energy functional of STF (19) is given by [45] (here we omit in our notation the t -dependence of h)

$$\frac{\delta E[h(x)]}{\delta h(x)} = \frac{4\pi^2}{3h(x)^3} - \frac{\partial^2 h(x)}{\partial x^2}. \quad (\text{B.1})$$

The Hessian we are looking for is formally the functional derivative of the functional derivative. If we rewrite equation (B.1) as an integral,

$$\frac{\delta E[h(x)]}{\delta h(x)} = F[h(x)] = \int_0^1 \left(\frac{4\pi^2}{3h(x')^3} - \frac{\partial^2 h(x')}{\partial x'^2} \right) \delta(x' - x) dx' \quad (\text{B.2})$$

$$= \int_0^1 f(x', h(x'), \frac{\partial^2 h(x')}{\partial x'^2}) dx', \quad (\text{B.3})$$

we can again use the definition of functional derivative [45] to get

$$\int_0^1 \frac{\delta F[h(x)]}{\delta h(x)} \xi(x) dx = \left\{ \frac{d}{d\epsilon} (F[h(x) + \epsilon \xi(x)]) \right\}_{\epsilon=0} \quad (\text{B.4})$$

$$= \int_0^1 \frac{\partial f}{\partial h} \xi(x') + \frac{\partial^2 f}{\partial (\partial_{x'}^2 h(x'))^2} \frac{\partial^2 \xi(x')}{\partial x'^2} dx' \quad (\text{B.5})$$

$$= \int_0^1 \xi(x') \left(\frac{\partial f}{\partial h} + \frac{\partial^2}{\partial x'^2} \frac{\partial^2 f}{\partial (\partial_{x'}^2 h(x'))^2} \right) dx' \quad (\text{B.6})$$

$$= \int_0^1 \xi(x') \left(-\frac{4\pi^2}{h(x')^4} \delta(x' - x) - \frac{\partial^2}{\partial x'^2} \delta(x' - x) \right) dx' \quad (\text{B.7})$$

$$= -\frac{4\pi^2}{h(x)^4} \xi(x) - \frac{\partial^2 \xi(x)}{\partial x^2} \quad (\text{B.8})$$

$$= \int_0^1 \frac{\delta^2 E[h(x)]}{\delta h(x)^2} \xi(x) dx. \quad (\text{B.9})$$

Here $\xi(x)$ is a periodic test function, the third line used integration by parts, and the fourth line used the properties of Dirac delta functional and its derivatives. The Hessian, $\delta^2 E[h(x)]/\delta h(x)^2$, can be interpreted as an operator on $\xi(x)$, and thus can be discretised and calculated numerically.

Similarly, we can calculate the gradient and the Hessian of the energy functional of the urban segregation model. Equations (22) and (5) give us the following energy functional

$$E[\rho] = \int_0^1 \left(\rho \log \rho + (1 - \rho) \log(1 - \rho) - \frac{1}{2} C \rho^2 - \frac{\kappa^2}{4} C \rho \frac{\partial^2 \rho}{\partial x^2} \right) dx. \quad (\text{B.10})$$

The functional derivative of $E[\rho]$ is

$$\frac{\delta E[\rho]}{\delta \rho} = \log(\rho) - \log(1 - \rho) - C \rho - \frac{\kappa^2}{2} C \frac{\partial^2 \rho}{\partial x^2}, \quad (\text{B.11})$$

or in its integral form

$$\frac{\delta E[\rho]}{\delta \rho} = F[\rho] = \int_0^1 f(x', \rho(x'), \frac{\partial^2 \rho(x')}{\partial x'^2}) \quad (\text{B.12})$$

$$= \int_0^1 \left(\log\left(\frac{\rho(x')}{1 - \rho(x')}\right) - C \rho(x') - \frac{\kappa^2}{2} C \frac{\partial^2 \rho(x')}{\partial x'^2} \right) \delta(x' - x) dx'. \quad (\text{B.13})$$

And the Hessian of $E[\rho]$ is given by

$$\int_0^1 \frac{\delta F[\rho(x)]}{\delta \rho(x)} \xi(x) dx = \int_0^1 \frac{\partial f}{\partial \rho} \xi(x') + \frac{\partial^2 f}{\partial (\partial_{x'}^2 \rho(x'))^2} \frac{\partial^2 \xi(x')}{\partial x'^2} dx' \quad (\text{B.14})$$

$$= \int_0^1 \xi(x') \left(\left(\frac{1}{\rho(x')} + \frac{1}{1 - \rho(x')} - C \right) \delta(x' - x) - \frac{\kappa^2}{2} C \frac{\partial^2}{\partial x'^2} \delta(x' - x) \right) dx' \quad (\text{B.15})$$

$$= \left(\frac{1}{\rho(x)} + \frac{1}{1 - \rho(x)} - C \right) \xi(x) - \frac{\kappa^2}{2} C \frac{\partial^2 \xi(x)}{\partial x^2} \quad (\text{B.16})$$

$$= \int_0^1 \frac{\delta^2 E[\rho(x)]}{\delta \rho(x)^2} \xi(x) dx. \quad (\text{B.17})$$

Appendix C. Local approximation of convolution

In this section we show the local approximation of convolution with a Gaussian kernel. Given a Gaussian kernel with variance κ^2 ,

$$K(x) = \frac{1}{\sqrt{2\pi\kappa}} \exp\left(-\frac{x^2}{2\kappa^2}\right), \quad (\text{C.1})$$

we first show that its Fourier transform is also a Gaussian, that is

$$\hat{K}(k) = \int_{-\infty}^{\infty} \exp(-ikx) K(x) dx = \exp\left(-\frac{\kappa^2 k^2}{2}\right). \quad (\text{C.2})$$

Differentiate the Gaussian kernel gives

$$\frac{dK}{dx} = -\frac{x}{\kappa^2} K(x). \quad (\text{C.3})$$

Fourier transform on both side gives

$$ik\hat{K}(k) = \frac{1}{i\kappa^2} \frac{d\hat{K}}{dk}, \quad (\text{C.4})$$

and so

$$\frac{1}{\hat{K}} \frac{d\hat{K}}{dk} = -k\kappa^2. \quad (\text{C.5})$$

Integrating both side from 0 to k gives

$$\ln(\hat{K}(k)) - \ln(\hat{K}(0)) = -\frac{k^2\kappa^2}{2}. \quad (\text{C.6})$$

Since the Gaussian kernel is normalised, we know that

$$\hat{K}(0) = \int_{-\infty}^{\infty} K(x) \exp(0) dx = 1, \quad (\text{C.7})$$

and so we have the desired result. Assuming $\kappa^2 \ll 1$, we can then Taylor expand $\hat{K} = 1 - \kappa^2 k^2/2 + \mathcal{O}(\kappa^4)$, and so

$$K(x) = \frac{1}{2\pi} \int_{-\infty}^{\infty} \hat{K}(k) \exp(ikx) dk = \frac{1}{2\pi} \int_{-\infty}^{\infty} \left(1 - \frac{\kappa^2}{2} k^2 + \mathcal{O}(\kappa^4)\right) \exp(ikx) dk. \quad (\text{C.8})$$

Since the Gaussian kernel is symmetric, the convolution is given by

$$K \star \rho = \int_{-\infty}^{\infty} \rho(y) K(x-y) dy \quad (\text{C.9})$$

$$= \int_{-\infty}^{\infty} \rho(y) \frac{1}{2\pi} \int_{-\infty}^{\infty} \left(1 - \frac{\kappa^2}{2} k^2 + \mathcal{O}(\kappa^4)\right) \exp(ik(x-y)) dk dy \quad (\text{C.10})$$

$$= \int_{-\infty}^{\infty} \frac{1}{2\pi} \hat{\rho}(k) \exp(ikx) dk - \frac{1}{2\pi} \int_{-\infty}^{\infty} \frac{\kappa^2}{2} k^2 \hat{\rho}(k) \exp(ikx) dk + \mathcal{O}(\kappa^4) \quad (\text{C.11})$$

$$= \rho(x) + \frac{\kappa^2}{2} \partial_x^2 \rho(x) + \mathcal{O}(\kappa^4). \quad (\text{C.12})$$